The Drosophila *attP40* docking site and derivatives are insertion mutations of MSP300

Kevin van der Graaf, Saurabh Srivastav, Pratibha Singh, James A McNew, and Michael Stern

Department of Biosciences, Program in Biochemistry and Cell Biology, Rice University, Houston, TX 77005

Corresponding author: Kevin van der Graaf

Department of Biosciences, Program in Biochemistry and Cell Biology, Rice University, Houston, TX 77005

Email: kv19@rice.edu

Phone: +1 713-348-3035

Kevin van der Graaf ORCID: https://orcid.org/0000-0002-2439-2227

Keywords

insertional mutation, ϕC31 docking site, nuclear clustering

Running Title

MSP300 insertional mutations by *attP40*

Abstract

The ϕC31 integrase system is widely used in *Drosophila* to allow transgene targeting to specific loci. Over the years, flies bearing any of more than 100 attP docking sites have been constructed. One popular docking site, termed *attP40*, is located close to the *Nesprin-1* orthologue *MSP300* and lies upstream of certain *MSP300* isoforms and within the first intron of others. Here we show that *attP40* causes larval muscle nuclear clustering, which is a phenotype also conferred by *MSP300* mutations. We also show that flies bearing insertions within *attP40* can exhibit decreased *MSP300* transcript levels in third instar larvae and, depending on the identity of the insertion, can exhibit inviability. These phenotypes do not require transcription from the insertions within *attP40*. These results demonstrate that *attP40* and insertion derivatives act as *MSP300* insertional mutations. These findings should be considered when interpretating data from *attP4*0-bearing flies.

Introduction

For several years, Drosophila investigators have used a genome integration method based on the site-specific ϕC31 integrase (Thorpe & Smith, 1998) to target transgenes to specific loci (Groth, 2004). With this method, ϕC31 integrase catalyzes sequence-directed recombination between a bacterial attachment site (attB, present within each of >100 attP "docking sites" in Drosophila) and a phage attachment site (attP, present within the integrating plasmid) (Thorpe et al., 2000; Bateman et al., 2006; Bischof et al., 2007; Groth & Calos, 2004; Venken et al., 2006). By allowing transgene insertion into specific, defined sequences (termed "docking sites), the ϕC31 integrase method increases the reproducibility and decreases the variability of transgene expression observed with the random transgene integration utilized by P elements.

Two docking sites, *attP2*, located at position 68A4 on chromosome III and *attP40*, located at position 25C on chromosome II, are widely used docking sites for LexA drivers and Gal4-driven Transgenic RNAi Project (TRiP) insertions (Zirin et al., 2020). These two *attP*

docking sites are favorable because they express inserted transgenes at high levels while maintaining low basal expression (Perkins et al., 2015). In fact, the Drosophila stock center at Bloomington, IN, reports possessing 16,503 Drosophila lines carrying *attP40* and 14,970 lines carrying *attP2*; most lines carry transgenic RNAi project (TRiP) insertions or the activation domains or DNA binding domains from the Janelia split-Gal4 collection (Annette Parks, personal communication). Although originally reported to be located in an intergenic region, between *CG14035* and *MSP300* (Markstein et al., 2008), *attP40* lies within the first intron of certain *Msp300* isoforms ((Larkin et al., 2021) FlyBase FB2022_02). This observation raises the possibility that *attP40* might act as an insertional mutation for *MSP300.* Indeed, it was previously reported that certain insertions into attP40 could cause spreading of the H3K27me3 mark over the large *MSP300* exon (De et al., 2019). Thus, transgenes inserted within the *attP40* docking site might affect expression of at least a subset of *MSP300* isoforms.

Muscle-specific protein 300 kDa (MSP300) is a nuclear-associated Nesprin1 orthologue and a component of the Linker of Nucleoskeleton and Cytoskeleton (LINC) complex (Kim et al., 2015; Volk, 1992). The C-terminal domain contains a Klarsicht/Anc1/Syne Homology (KASH) domain that interacts with Sad1p/UNC-84 (SUN)- domain-containing proteins, connecting the outer and inner nuclear membranes (Xie and Fischer, 2008; McGee et al., 2006). In Drosophila larvae, *MSP300* transcription has been reported in muscle (Volk, 1992) and fat body (Zheng et al., 2020). In larval muscle, MSP300 forms striated F-actin-based filaments that lie between muscle nuclei and postsynaptic sites at the neuromuscular junction. MSP300 also wraps around immature boutons in response to electrical activity and is required for postsynaptic RNA localization and synaptic maturation (Packard et al., 2015). MSP300 is also required for normal nuclear localization in muscle cells and for integrity of muscle cell insertion sites into the cuticle (Volk, 1992; Volk, 2013; Zhang et al., 2010). MSP300 isoforms lacking the KASH domain confer deficits in larval locomotion, localization of the excitatory neurotransmitter receptor GluRIIA at the neuromuscular junction (NMJ), and proper NMJ functioning, independently of its role in muscle nuclear positioning (Morel et al., 2014). Non-

muscle deficits conferred by *MSP300* mutations include defects in oocyte development and female fertility (Yu et al., 2006). In humans, mutations in the Nesprin family are associated with several musculoskeletal disorders, including bipolar disorder, autosomal recessive cerebellar ataxia type 1 (ARCA1), X-linked Emery-Dreifuss muscular dystrophy (EDMD) and are risk factors for schizophrenia and autism (Rajgor & Shanahan, 2013).

Here, we show that flies carrying *attP40* site exhibit a weak nuclear clustering phenotype in *Drosophila* larval muscle, which suggests that *attP40* is an *MSP300* insertional mutation. Further, we show that inserting transgenes into *attP40* can increase severity of the nuclear clustering phenotype. We use quantitative RT-PCR (Q-PCR) to show that insertions within *attP40* decrease *MSP300* transcript levels in 3rd instar larvae. Finally, we show that several transgene insertions into *attP40*, particularly those constructed from the *Valium 20* vector (Perkins et al., 2015), confer recessive lethality. Because of the variable effects of different transgene insertions into *attP40*, investigators should use caution in interpreting data collected from *Drosophila* carrying these insertions.

Materials and Methods

Drosophila stocks

All fly stocks were maintained on standard cornmeal/agar *Drosophila* media: 69.1 g/l corn syrup, 9.6 g/l soy flour, 16.7 g/l yeast, 5.6 g/l agar, 70.4 g/l cornmeal, 4.6 ml/l propionic acid and 3.3 gm/l nipagin. Flies carrying *attP2* and *attP40* lacking insertions were retrieved as white-eyed progeny from transgene insertions carried out at GenetiVision (Houston, TX). The *Drosophila* Stock Center at Bloomington, Indiana provided *TRiP JNK* (#57035), *TRiP Spatacsin* (#64868), *TRiP atl* (#36736), *TRiP Mcu* (#42580), *13XLexAop2-IVS-myr::GFP*, *LexA::Mef2* (#61543) and *LexA::nSyb* (#52817). All experiments were performed on *Drosophila* that had been reared and maintained at room temperature (22^{o}C) with a 12h: 12h light:dark cycle unless otherwise indicated.

Immunocytochemistry

All larvae were dissected in HL3.1 (Feng et al., 2004) in a magnetic chamber, and fixed in 4% paraformaldehyde for 10 minutes, then washed in PBS with 0.3% Triton-X (PBS-T) and blocked for 30 minutes in PBS-T with 1% BSA. Samples were incubated overnight at 4^{o}C with primary antibody, washed thoroughly with PBS-T and then incubated for 2.5 hours at room temperature with secondary antibody. Samples were then washed with PBS-T and mounted in VectaShield Antifade Mounting Medium containing DAPI (Vector laboratories; H-1200-10).

The primary antibody used was mouse anti-Lamin (ADL67.10, 1:100) from the Developmental Studies Hybridoma Bank (DSHB). We used goat anti-mouse IgG antibody coupled with Alexa-Fluor-488 (Abcam, ab6785) for the secondary antibody. Alexa Fluor® 647 phalloidin (1:200) was used to visualize F-actin. All images were acquired on a Zeiss LSM800 with an Airyscan confocal microscope.

Nuclear clustering analysis

Third instar larval body wall muscle 6 was chosen for all nuclear clustering analysis. Images were opened in ImageJ and nuclei clusters in muscle 6 were counted. We defined a “cluster” as two or more nuclei in which the distance between two nuclear borders was less than five microns. We analyzed six larvae from hemisegments A2-A4 (18 hemisegments total) for each genotype.

Microsoft excel was used to import all nuclear clustering data. “Normal” muscles contained no clusters. For muscles that contained cluster(s), we determined cluster number and nuclei number per cluster. All data were plotted on a column graph using GraphPad Prism v9.3.1.

Quantitative RT-PCR

Primers were designed with PrimerBLAST software according to the published sequence of *MSP300*. The 3’end region, which includes the KASH domain, within *MSP300* was chosen for transcriptional analysis (Figure 2A red arrows). The *MSP300* forward primer

sequence was 5'-TCAACCTCTTCCAATGCAGGC-3', and the *MSP300* reverse primer sequence was 5'-CGCCAGAACCGTGGTATTGA-3'. For amplification of *Rp49,* chosen as the housekeeping gene, the forward primer sequence was 5'-TGTCCTTCCAGCTTCAAGATGACCATC-3' and the reverse primer sequence was 5'-CTTGGGCTTGCGCCATTTGTG-3'. Total RNA (500 ng) was extracted from frozen whole larvae with Direct-zol™ RNA MicroPrep (Zymo Research) according to manufacturer's protocol. The yield of RNA was estimated with the Nanodrop2000 (ThermoFisher). The A_{260}:A_{280} ratio was between 1.8-2.1. Superscript™ III First-Strand Synthesis System (ThermoFisher) was used to generate cDNA according to manufacturer's protocol. Reverse transcribed cDNA was then amplified in a 20 µl PCR reaction by the ABI Prism 7000 system (Applied Biosystems) with the universal conditions: 50°C for 2 min, 95°C for 10 min, and 40 cycles (15s at 95°C, 1 min at 60°C). Each sample contained 10 whole larvae. Three separate biological samples were collected from each genotype, and triplicate measures of each sample were conducted for amplification consistency. Data were analyzed with the relative $2^{-\Delta\Delta Ct}$ method to ensure consistency (Livak & Schmittgen, 2001).

Statistical analysis

For all statistical analysis, an unpaired student's T-test was performed. A two-tailed analysis was performed with a 95% confidence level. All statistical tests were performed in GraphPad Prism v9.3.1.

Availability

Fly stocks are available upon request. The authors affirm that all data necessary for confirming the conclusions of the article are present within the article and figures.

Results

The presence of *attP40* causes clustering of nuclei in larval muscles

attP2 and *attP40* are two widely used *attP* docking sites in *Drosophila* for insertions of LexA drivers, Gal4-driven *TRiP* insertions, and other constructs. Both docking sites provide high levels of induced transgene expression while maintaining low basal expression. As of February 2022, the Bloomington Drosophila Stock Center (Bloomington, IN) provides 16,503 stocks carrying *attP40* and 14,941 stocks carrying *attP2* (Annette Parks, personal communication). We noticed abnormalities in nuclear positioning in larval body wall muscles from flies carrying *attP40* vs. flies carrying *attP2*, or vs. flies lacking *attP* insertions (Figure 1A-E).

The *attP40* docking site is located within or upstream of *MSP300*, depending on isoforms

To investigate further the *attP40* nuclear clustering phenotype, we looked more closely at the *attP40* chromosomal location. The gene nearest *attP40*, *MSP300*, is predicted to express 11 different isoforms. *attP40* lies within intron 1 for transcripts RH, RI, RJ and RK and upstream of transcripts RB, RD, RE, RF, RG, RL and RM (Figure 2A). These results raise the possibility that *attP40* could affect *MSP300* transcript levels. Indeed, De et al. (De et al., 2019) reported that certain transgene insertions into *attP40* alter the H3K27me3 epigenetic mark over at least a part of *MSP300*. Given previous reports that *MSP300* variants alter muscle myonuclear spacing (Elhanany-Tamir et al., 2012; Volk, 1992), a phenotype similar to what we observe in flies carrying *attP40*, we hypothesize that *attP40* affects larval muscle nuclear clustering by affecting *MSP300* expression.

Inserting transgenes into attP40 increases phenotypic severity

We tested if introducing insertions into *attP40* could affect the muscle nuclear clustering phenotype. Figure 2B shows a schematic of ϕC31-mediated generation of insertions within

attP40. Figures 2C and 2D represent an overview of all genotypes used in this paper. Representative images of larval muscle nuclear position from indicated genotypes are shown in Figure 3 (A-G). The number of normal hemisegments from each genotype are shown in Figure 3I, whereas the number of nuclei within each cluster from each genotype are shown in Figure 3J.

Larvae from the *attP2* control line show a high percentage of normal hemisegments with very little nuclear clustering (Figure 3A and Figures 3I and 3J column 1), whereas *attP40*-carrying larvae show few normal hemisegments and a clear nuclear clustering phenotype (Figure 3B and Figures 3I and 3J column 2). To determine if insertions into *attP40* could affect nuclear clustering, we crossed *attP40* flies with flies bearing the functionally neutral *LexA-IVS-myr::GFP* inserted into *attP40*, and found that presence of *LexA-IVS-myr::GFP* caused the appearance of extremely large nuclear clusters (containing up to 12 nuclei), which were not observed in *attP40* (Figure 3B and Figures 3I and 3J, column 4) and indicate phenotypic enhancement by *LexA-IVS-myr::GFP.* To determine if Gal4-regulated transgenes inserted into *attP40* would likewise enhance the nuclei clustering phenotype, we crossed *attP40* flies to flies carrying either of two Gal4-driven shRNA constructs, targeting *JNK* or *Spatacsin* (CG13531) created by the transgenic RNAi project (Perkins et al., 2015). We found that *TRiP Spatacsin/attP40* larvae displayed a nuclear clustering phenotype intermediate between *LexAop-IVS-myr::GFP/attP40* and *attP40* (Figures 3I and 3J, columns 2 and 4 vs. 7). *TRiP JNK/attP40*, in contrast, displayed a nuclear clustering phenotype intermediate between *attP40* and *attP2* (Figures 3I and 3J, columns 1 and 2 vs. 8). The phenotypic difference *TRiP JNK/attP40* and *TRiP Spatacsin/attP40* was surprising, as both *TRiP* insertions carry the same *Valium 20* vector inserted into *attP40*. This phenotypic difference could reflect differences in the precise shRNA sequence within *Valium 20*, or differences in genetic background.

To determine if inserting a transgene into both *attP40* homologues would affect nuclear clustering, we crossed flies bearing the neutral reporter *LexAop-IVS-myr::GFP* to flies bearing *LexA::nSyb*. We found that these *LexAop-IVS-myr::GFP/LexA::nSyb* larvae exhibited a

nuclear clustering phenotype similar to *attP40* larvae (Figures 3 I and 3J columns 2 vs. 6). Thus, inserting a transgene into the second *attP40* homologue did not increase phenotypic severity.

It was previously reported (De et al., 2019) that certain transgene insertions into *attP40* could generate epigenetic marks that spread into *MSP300*, potentially altering *MSP300* expression. To determine if expressing transgene insertions into *attP40* would affect nuclear clustering, we created larvae in which transgene insertions into each *attP40* would be expressed in muscle. We found that these *LexAop-IVS-myr::GFP/LexA::Mef2* larvae showed a more severe nuclear clustering phenotype *LexAop-IVS-myr::GFP/LexA::nSyb* (Figure 3E and Figures 3I and 3J column 5), and was the only genotype tested that exhibited no muscles with normal nuclear positioning. This observation is consistent with the possibility that the transcription of *attP40* insertions might increase severity of nuclear clustering phenotype.

To determine if nuclear clustering required *attP40* inserted into both homologues, we tested the effects on nuclear clustering in *LexAop-IVS-myr::GFP/+; +/attP2* larvae. We found that these larvae exhibit a phenotype very similar to the control *attP2* larvae (Figure 3C and Figures 3I and 3J, column 3). Thus, the *attP40* acts like a recessive *MSP300* insertion mutation.

Effects of *attP40* and derivatives on *MSP300* transcript levels

We hypothesized that nuclei clustering in larvae homozygous for *attP40* and derivatives reflected altered expression of at least some of the eleven *MSP300* isoforms (Figure 2A). To test this hypothesis, we prepared RNA from whole third instar larvae and performed quantitative RT-PCR (Q-PCR) using primers from the far 3' end of *MSP300*. This region of *MSP300* would account for most of the annotated isoforms, and included the KASH domain ((Xie & Fischer, 2008); Figure 2A). We found that *MSP300* transcript levels were decreased about two-fold in all genotypes tested in which at least one transgene was inserted into *attP40* (Figure 4). These results support the possibility that *attP40* derivatives cause nuclei clustering

by decreasing *MSP300* transcription. The observation that larvae homozygous for *attP40* exhibited wildtype levels of *MSP300* transcripts, despite exhibiting a strong nuclear clustering phenotype, seems inconsistent with this view. However, we note that *MSP300* is transcribed in larval fat bodies as well as muscle (Zheng et al., 2020). Because fat body transcripts are included in our RNA samples for Figure 4, if *attP40* decreases *MSP300* in muscle but not fat body, decreased *MSP300* transcript levels taken from whole larvae might not be apparent. Further analysis of this possibility is beyond the scope of this paper.

Effects of *attP40* and derivatives on viability and fertility

Flies homozygous for *attP40* exhibited varying degrees of viability deficits. In particular, we were unable to obtain adults homozygous for three *TRiP* constructs inserted into *attP40*: *TRiP atl*, *TRiP Mcu,* and *TRiP Spatacsin (CG13531)*. We were unable to separate the recessive lethality from the insertion for *TRiP atl* by recombination, indicating the recessive lethal mutation was at, or linked to, the *TRiP atl* insertion. However, flies homozygous for *TRiP JNK* were viable and fertile, indicating that not all *TRiP Valium 20* insertions into *attP40* were lethal.

Discussion

Effects of the *attP40* docking site and derivatives on *MSP300*-mediated phenotypes

The *attP40* docking site for Drosophila transgene integration is widely used for ϕC31-mediated transgene integration. *attP40* lies within the transcription unit of *MSP300*, which encodes the Drosophila orthologue of Nesprin-1; this observation raises the possibility that *attP40* is an *MSP300* insertional mutation. Here we show that *attP40*, either alone or containing any of several specific transgene insertions, causes phenotypes similar to *MSP300* mutations, such as larval muscle nuclear clustering and viability deficits. In addition, larvae with transgene

insertions within *attP40* exhibit an approximately two-fold decrease in *MSP300* transcript levels. The effect on nuclear clustering and viability varies depending on the precise transgene introduced into *attP40*. We conclude that *attP40* is an insertional mutation for *MSP300*.

attP40 is recessive for phenotypes tested

We tested if *attP40* and derivatives containing insertions into *attP40* were recessive or dominant for the nuclear clustering and *MSP300* transcription phenotypes. We found that flies bearing the neutral reporter *LexA-myr-GFP* within *attP40* exhibited severe nuclear clustering and decreased *MSP300* when in combination with *attP40*-bearing flies, but were phenotypically wildtype in, when in combination with *attP2*. We conclude that *attP40* and its insertional derivatives are recessive for nuclear clustering and *MSP300* transcription phenotypes.

Effects of specific transgene insertions into *attP40* on mutant phenotypes

We tested if the molecular nature of specific transgenes inserted into *attP40* would affect mutant phenotypes. First, we found that transgenes from either the *LexA* or the *Gal4* regulatory systems were capable enhancing the nuclear positioning phenotype and decreasing *MSP300* transcript levels. Second, we tested if transcription of inserted transgenes in muscle would affect mutant phenotypes. In particular, we compared nuclear positioning in larvae expressing *LexA-myr-GFP* in neurons vs. muscle and found that muscle expression modestly increased severity of the nuclear clustering phenotype but did not affect *MSP300* transcript levels. These results indicate that muscle transcription of inserted transgenes is not necessary for mutant phenotype, but we are unable to rule out the possibility muscle transcription could contribute to severity of mutant phenotype. Third, we found that several *TRiP* inserts constructed from the *Valium 20* vector (Ni et al., 2008; Ni et al., 2009; Ni et al., 2011) exhibited recessive lethality. For the *TRiP atl* insert, we were unable to separate this lethality from the

insertion, indicating that the recessive lethality lies within, or close to, the insertion. However, not all *Valium 20 TRiP* insertions conferred recessive lethality, as flies bearing the *TRiP JNK* insertion are viable and fertile. The reason that fly viability appears to be especially sensitive to *Valium 20* derivatives inserted into *attP40*, or why different *TRiP* insertions confer different viability defects, remains unclear.

Conclusions

We have shown *attP40* and derivatives containing insertions confer *MSP300* mutant phenotypes and can decrease *MSP300* transcript levels. Investigators should use caution when interpreting data resulting from flies containing *attP40*.

Acknowledgments

The authors would like to thank the Bloomington Stock Center for providing all the fly lines used in this study. This study is funded by grants R01 NS102676 and R21 NS111340 to MS and JAM. We are grateful to Alekhya Gurram for assistance with Q-PCR experiments.

The authors declare that they have no conflicts of interest with the contents of this article.

References

Bateman, J. R., Lee, A. M., & Wu, C. (2006). Site-Specific Transformation of Drosophila via ϕC31 Integrase-Mediated Cassette Exchange. *Genetics*, *173*(2), 769–777. https://doi.org/10.1534/genetics.106.056945

Bischof, J., Maeda, R. K., Hediger, M., Karch, F., & Basler, K. (2007). An optimized transgenesis system for Drosophila using germ-line-specific C31 integrases. *Proceedings of the National Academy of Sciences*, *104*(9), 3312–3317. https://doi.org/10.1073/pnas.0611511104

De, S., Cheng, Y., Sun, M., Gehred, N. D., & Kassis, J. A. (2019). Structure and function of an ectopic Polycomb chromatin domain. *Science Advances*, *5*(1), eaau9739. https://doi.org/10.1126/sciadv.aau9739

Elhanany-Tamir, H., Yu, Y. V., Shnayder, M., Jain, A., Welte, M., & Volk, T. (2012). Organelle positioning in muscles requires cooperation between two KASH proteins and microtubules. *Journal of Cell Biology*, *198*(5), 833–846. https://doi.org/10.1083/jcb.201204102

Feng, Y., Ueda, A., & Wu, C.-F. (2004). A modified minimal hemolymph-like solution, HL3.1, for physiological recordings at the neuromuscular junctions of normal and mutant Drosophila larvae. *Journal of Neurogenetics*, *18*(2), 377–402. https://doi.org/10.1080/01677060490894522

Groth, A. C. (2004). Construction of Transgenic Drosophila by Using the Site-Specific Integrase From Phage C31. *Genetics*, *166*(4), 1775–1782. https://doi.org/10.1534/genetics.166.4.1775

Groth, A. C., & Calos, M. P. (2004). Phage Integrases: Biology and Applications. *Journal of Molecular Biology*, *335*(3), 667–678. https://doi.org/10.1016/j.jmb.2003.09.082

Kim, D. I., Birendra, K. C., & Roux, K. J. (2015). Making the LINC: SUN and KASH protein interactions. *Biological Chemistry*, *396*(4), 295–310. https://doi.org/10.1515/hsz-2014-0267

Larkin, A., Marygold, S. J., Antonazzo, G., Attrill, H., dos Santos, G., Garapati, P. V, Goodman, J. L., Gramates, L. S., Millburn, G., Strelets, V. B., Tabone, C. J., Thurmond, J., & FlyBase Consortium. (2021). FlyBase: updates to the Drosophila melanogaster knowledge base. *Nucleic Acids Research*, *49*(D1), D899–D907. https://doi.org/10.1093/nar/gkaa1026

Livak, K. J., & Schmittgen, T. D. (2001). Analysis of Relative Gene Expression Data Using Real-Time Quantitative PCR and the 2−ΔΔCT Method. *Methods*, *25*(4), 402–408. https://doi.org/10.1006/meth.2001.1262

Markstein, M., Pitsouli, C., Villalta, C., Celniker, S. E., & Perrimon, N. (2008). Exploiting position effects and the gypsy retrovirus insulator to engineer precisely expressed transgenes. *Nature Genetics*, *40*(4), 476–483. https://doi.org/10.1038/ng.101

McGee, M. D., Rillo, R., Anderson, A. S., & Starr, D. A. (2006). UNC-83 Is a KASH Protein Required for Nuclear Migration and Is Recruited to the Outer Nuclear Membrane by a Physical Interaction with the SUN Protein UNC-84. *Molecular Biology of the Cell*, *17*(4), 1790–1801. https://doi.org/10.1091/mbc.e05-09-0894

Morel, V., Lepicard, S., Rey, A. N., Parmentier, M.-L., & Schaeffer, L. (2014). Drosophila

Nesprin-1 controls glutamate receptor density at neuromuscular junctions. *Cellular and Molecular Life Sciences : CMLS*, *71*(17), 3363–3379. https://doi.org/10.1007/s00018-014-1566-7

Ni, J.-Q., Liu, L.-P., Binari, R., Hardy, R., Shim, H.-S., Cavallaro, A., Booker, M., Pfeiffer, B. D., Markstein, M., Wang, H., Villalta, C., Laverty, T. R., Perkins, L. A., & Perrimon, N. (2009). A Drosophila resource of transgenic RNAi lines for neurogenetics. *Genetics*, *182*(4), 1089–1100. https://doi.org/10.1534/genetics.109.103630

Ni, J.-Q., Markstein, M., Binari, R., Pfeiffer, B., Liu, L.-P., Villalta, C., Booker, M., Perkins, L., & Perrimon, N. (2008). Vector and parameters for targeted transgenic RNA interference in Drosophila melanogaster. *Nature Methods*, *5*(1), 49–51. https://doi.org/10.1038/nmeth1146

Ni, J.-Q., Zhou, R., Czech, B., Liu, L.-P., Holderbaum, L., Yang-Zhou, D., Shim, H.-S., Tao, R., Handler, D., Karpowicz, P., Binari, R., Booker, M., Brennecke, J., Perkins, L. A., Hannon, G. J., & Perrimon, N. (2011). A genome-scale shRNA resource for transgenic RNAi in Drosophila. *Nature Methods*, *8*(5), 405–407. https://doi.org/10.1038/nmeth.1592

Packard, M., Jokhi, V., Ding, B., Ruiz-Cañada, C., Ashley, J., & Budnik, V. (2015). Nucleus to Synapse Nesprin1 Railroad Tracks Direct Synapse Maturation through RNA Localization. *Neuron*, *86*(4), 1015–1028. https://doi.org/10.1016/j.neuron.2015.04.006

Perkins, L. A., Holderbaum, L., Tao, R., Hu, Y., Sopko, R., McCall, K., Yang-Zhou, D., Flockhart, I., Binari, R., Shim, H.-S., Miller, A., Housden, A., Foos, M., Randkelv, S., Kelley, C., Namgyal, P., Villalta, C., Liu, L.-P., Jiang, X., … Perrimon, N. (2015). The Transgenic RNAi Project at Harvard Medical School: Resources and Validation. *Genetics*, *201*(3), 843–852. https://doi.org/10.1534/genetics.115.180208

Rajgor, D., & Shanahan, C. M. (2013). Nesprins: from the nuclear envelope and beyond. *Expert Reviews in Molecular Medicine*, *15*, e5. https://doi.org/10.1017/erm.2013.6

Thorpe, H. M., & Smith, M. C. M. (1998). In vitro site-specific integration of bacteriophage DNA catalyzed by a recombinase of the resolvase/invertase family. *Proceedings of the National Academy of Sciences*, *95*(10), 5505–5510. https://doi.org/10.1073/pnas.95.10.5505

Venken, K. J. T., He, Y., Hoskins, R. A., & Bellen, H. J. (2006). P[acman]: A BAC Transgenic Platform for Targeted Insertion of Large DNA Fragments in D. melanogaster. *Science*, *314*(5806), 1747–1751. https://doi.org/10.1126/science.1134426

Volk, T. (1992). A new member of the spectrin superfamily may participate in the formation of embryonic muscle attachments in Drosophila. *Development (Cambridge, England)*, *116*(3), 721–730. https://cob.silverchair-cdn.com/cob/content_public/journal/dev/116/3/10.1242_dev.116.3.721/1/721.pdf?Expires=1637262326&Signature=tXQOzf8kOI1O7fLcIN1uELSJle0OY1D5WhqN0birNEFfSH9D0rFuZTZebb0bKSXb87howt4ksnDBX40L~pGdmcYaVcmRNplPPQnEfmvZVAuWxxytBbvo~0~A15Zip

Volk, Talila. (2013). Positioning nuclei within the cytoplasm of striated muscle fiber. *Nucleus*, *4*(1), 18–22. https://doi.org/10.4161/nucl.23086

Xie, X., & Fischer, J. A. (2008). On the roles of the Drosophila KASH domain proteins Msp-300 and Klarsicht. *Fly*, *2*(2), 74–81. https://doi.org/10.4161/fly.6108

Yu, J., Starr, D. A., Wu, X., Parkhurst, S. M., Zhuang, Y., Xu, T., Xu, R., & Han, M. (2006). The KASH domain protein MSP-300 plays an essential role in nuclear anchoring during

Drosophila oogenesis. *Developmental Biology*, *289*(2), 336–345. https://doi.org/10.1016/j.ydbio.2005.10.027

Zhang, J., Felder, A., Liu, Y., Guo, L. T., Lange, S., Dalton, N. D., Gu, Y., Peterson, K. L., Mizisin, A. P., Shelton, G. D., Lieber, R. L., & Chen, J. (2010). Nesprin 1 is critical for nuclear positioning and anchorage. *Human Molecular Genetics*, *19*(2), 329–341. https://doi.org/10.1093/hmg/ddp499

Zheng, Y., Buchwalter, R. A., Zheng, C., Wight, E. M., Chen, J. V, & Megraw, T. L. (2020). A perinuclear microtubule-organizing centre controls nuclear positioning and basement membrane secretion. *Nature Cell Biology*, *22*(3), 297–309. https://doi.org/10.1038/s41556-020-0470-7

Zirin, J., Hu, Y., Liu, L., Yang-Zhou, D., Colbeth, R., Yan, D., Ewen-Campen, B., Tao, R., Vogt, E., VanNest, S., Cavers, C., Villalta, C., Comjean, A., Sun, J., Wang, X., Jia, Y., Zhu, R., Peng, P., Yu, J., … Perrimon, N. (2020). Large-Scale Transgenic Drosophila Resource Collections for Loss- and Gain-of-Function Studies. *Genetics*, *214*(4), 755–767. https://doi.org/10.1534/genetics.119.302964

Author Contributions

KvdG – Collected the data, designed the analysis, performed the analysis, wrote manuscript, edited the manuscript; SS – performed the analysis; PS – performed the analysis; MS – Conceived and designed the analysis, edited the manuscript; JAM – Conceived and designed the analysis.

Figures

Figure 1

Nuclear clustering observed in *attP40* larval muscles. A-D) Representative images of third instar larval muscle 6 of the indicated genotypes. Nuclei were visualized with DAPI (blue) and actin was visualized with phalloidin (magenta). Muscle 6 was outlined with dotted white line. Dotted red lines indicate nuclear clusters. E) Schematic representation of nuclear clustering in muscle 6. If borders between two nuclei are less than 5 µm apart it is counted as a cluster (dotted red lines). Scale bar = 50 µm.

Figure 2

Overview of genotypes used for nuclear clustering study. A) The *Msp300* transcription unit. The *attP40* docking site is indicated with dotted line, the KASH domain with black arrow, and the location of PCR primer with red arrows in inset. B) Visual representation of the ϕC31 integrase system in *Drosophila*. The blue arrowhead represents the *attP* docking site of the chromosome and the red arrowhead represents the *attB* site present in the donor plasmid. The brown rectangle represents an insertion, and the hybrid sites resulting from a plasmid insertion are indicated as *attL* and *attR*. C) *attP40* shown as a blow arrowhead, *attP2* is shown as a green arrowhead. D) Representation of the different genotypes used in this study.

Figure 3

Clustering of nuclei in *attP40* larval muscles. A-H) Representative images of nuclei from third instar larval muscle 6 of the indicated genotypes. Dotted white lines show muscle outline. Nuclei were visualized with DAPI (blue) and anti-Lamin (green). Muscle 6 is outlined with a white-dotted line. I) Percentage of normal hemisegments (Y axis) in larvae of the indicated genotypes (X axis) (N=18 hemisegments from 6 larvae per genotype). J) Overview of cluster size and cluster count observed within 18 hemisegments for each genotype.

Figure 4

Effect of *attP40* and derivatives on *MSP300* transcript levels. Quantitative RT-PCR was used to measure *MSP300* transcript levels, normalized to *attP2* (Y axis), from whole third instar larvae of the indicated genotypes (X axis). Mean ± SEM was determined from at least three separate biological samples collected from each genotype, and triplicate measures of each sample. The $2^{-\Delta\Delta Ct}$ was employed for this measurement. Each sample contained a mix of 10 whole larvae.

Figure 1

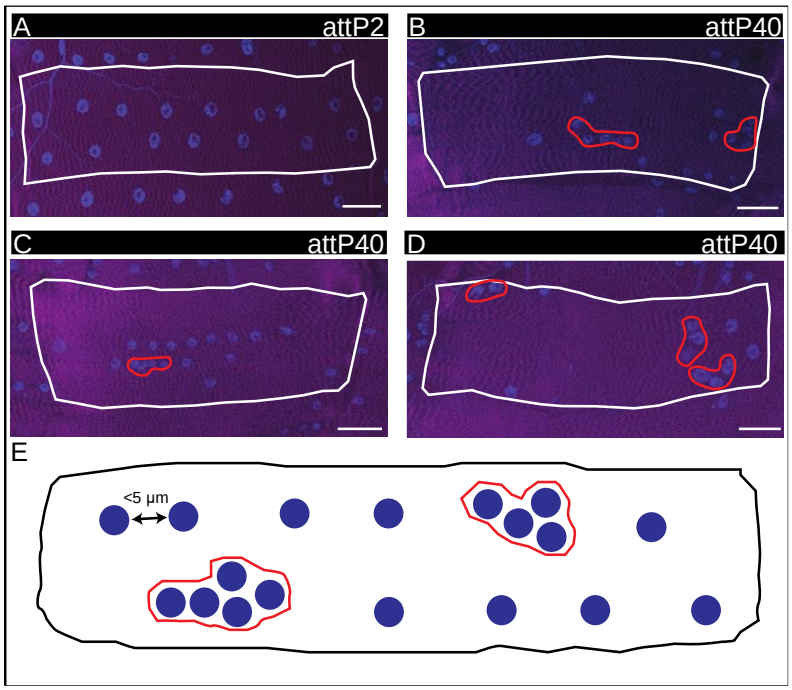

Figure 2

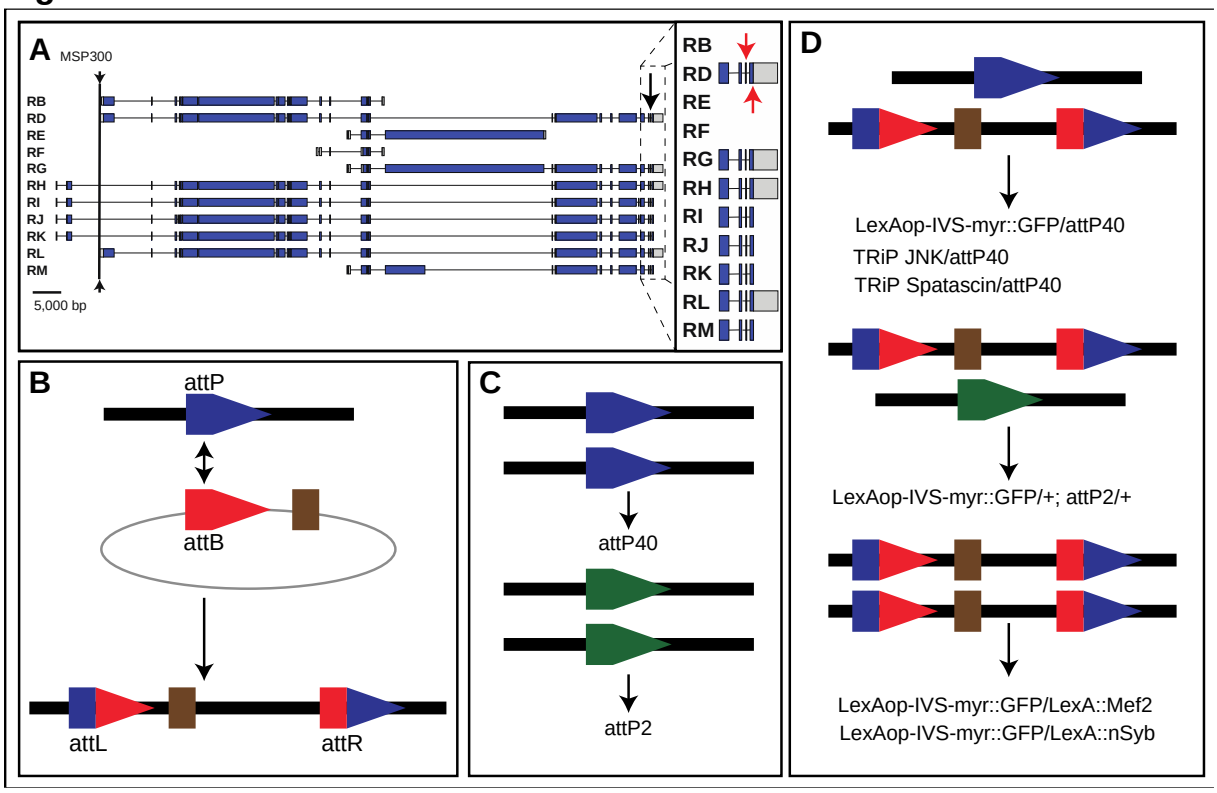

Figure 3

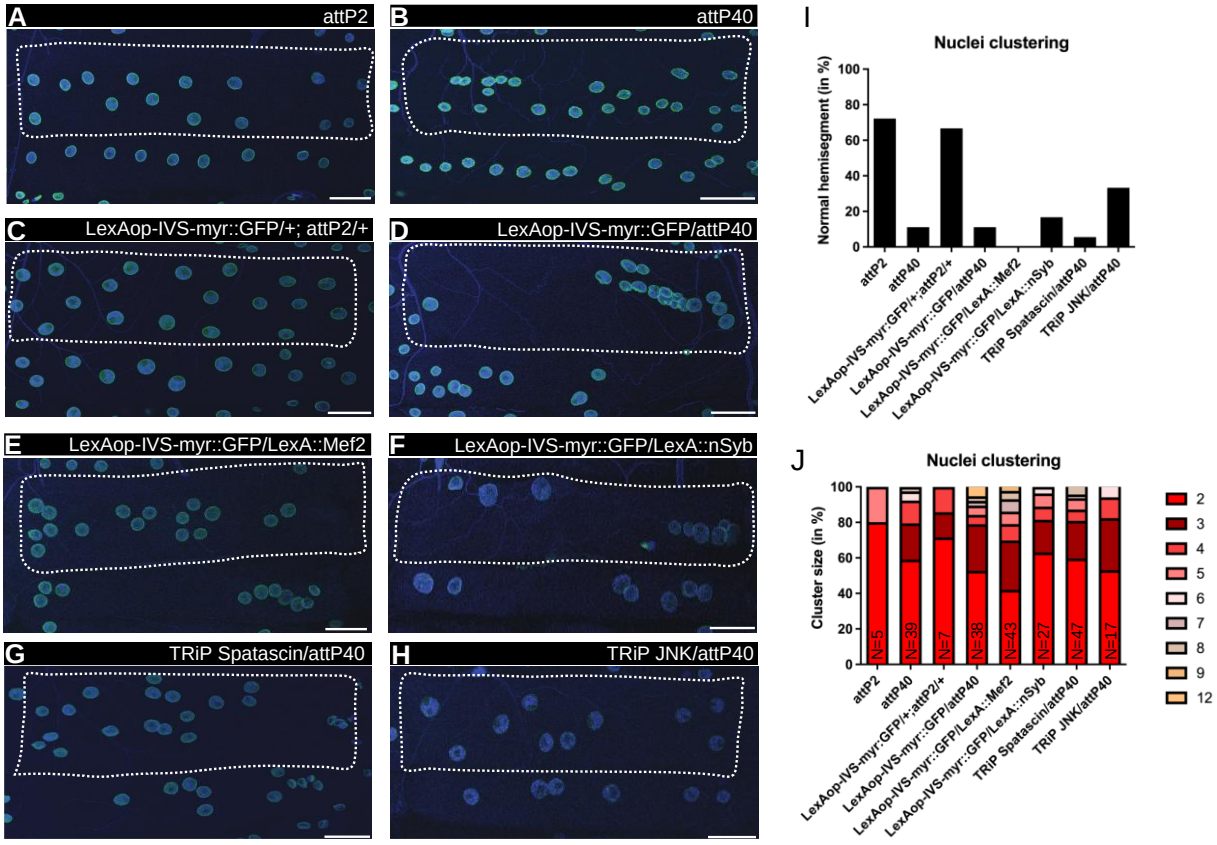

Figure 4